

---

# Evolutionary self-consistent models of HII galaxies

M. Martín Manjón<sup>1</sup>, M. Mollá<sup>2</sup> and A.I. Díaz<sup>3</sup>

<sup>1</sup> Universidad Autónoma de Madrid [mariluz.martin@uam.es](mailto:mariluz.martin@uam.es)

<sup>2</sup> CIEMAT [mercedes.molla@ciemat.es](mailto:mercedes.molla@ciemat.es)

<sup>3</sup> Universidad Autónoma de Madrid [angeles.diaz@uam.es](mailto:angeles.diaz@uam.es)

We have studied the viability of new theoretical models which combine a chemical evolution code, an evolutionary synthesis code and a photoionization code, to understand the star formation and evolution of HII galaxies. The emission lines observed in HII galaxies are reproduced by means of the photoionization code CLOUDY, using as ionizing spectrum the spectral energy distribution of the modeled HII galaxy, which, in turn, is calculated according to a Star Formation History (SFH) and a metallicity evolution given by a chemical evolution model. Our technique reproduces the observed diagnostic diagrams and equivalent width-color correlations for local HII galaxies.

## 1 Introduction

Blue Compact Galaxies (BCG), specially HII galaxies, are gas rich dwarf galaxies which, according to the observed strong and narrow emission lines that dominate their optical spectra, are experiencing intense star formation processes in very reduced volumes. These emission lines are produced by massive stars that ionize the surrounding gas which implies the existence of a very young stellar population. On the other hand, the analysis of their emission line spectra shows that HII galaxies are very metal poor systems. These two facts taken together lead to the idea that actually these systems were very young objects experiencing their first burst of star formation [15]. However, recent photometric observations indicate that they host stellar populations which are at least  $10^7 - 10^8$  years old, reaching even 1 Gyr in some cases [7, 17, 1, 16]. At present, there seems to be a general agreement about the presence of underlying populations with ages of several Gyrs in BCGs and/or HII galaxies, that is, about the non existence of genuinely young galaxies in our local universe, but there is no consensus about how these stars formed.

There are some works that combine stellar synthesis techniques with photo-ionization codes ([5]). The synthesis models assume that a certain mass of stars is created in a single burst of formation, what implies that all stars

are similarly old and have similar metal composition. These generations of stars are called *Single Stellar Populations* (SSP). These models obtain as a result the spectral energy distribution of the population (SED) as the sum of the spectra of each individual star. After computing this SED, it is included in a photo-ionization code as the ionization source to compute the emission line spectrum. The addition of the chemical evolution allows to follow the metallicity of successive stellar generations. To our knowledge, a combination of chemical evolution, evolutionary population synthesis and photo-ionization models has not yet been attempted to analyze the BCG or HII galaxies. The potential of the method resides in the simultaneous use of the available information about the SFH, the photometric evolution and ionizing properties of the object: chemical abundances, SED or colors and emission line intensities. In this contribution we show that some of these models can adequately reproduce these constraints.

## 2 The models

The aim of this work is to check the possibility to face the problem of analyzing the HII galaxies data through the combination of the three techniques mentioned above in a self-consistent way, that is using the same assumptions about stellar evolution, stellar atmospheres and nucleosynthesis, and using a realistic age-metallicity relation. The procedure is to first compute chemical evolution models ([2, 9, 10]) which reproduce the observed chemical abundances and derive the SFH and the age-metallicity relation that is then in the computation, by means of evolutionary synthesis models, of the corresponding SED's ([5, 11]). Finally, we use the photo-ionization code CLOUDY (Ferland, 1991) using as inputs the calculated abundances and the synthesized spectra, to obtain the emission line intensities of the ionized gas. The combination of the results from spectrophotometric and photo-ionization models is used to calculate the line equivalent widths. The self-consistency and evolutionary nature of the models permit to calculate any quantity as a function of time, allowing their application to objects at different redshift.

We have run models starting with a total mass of gas of  $100 \cdot 10^6 \text{ M}_{\odot}$  concentrated inside a spherical volume radius of 500 pc. This is the characteristic size of starbursts in HII galaxies measured on CCD images [13]. We have assumed star formation to proceed in 10 consecutive bursts along 13.2 Gyrs, one every 1.3 Gyr. In every star formation episode, gas is consumed at a rate that depends on the available gas, being a decreasing function of time through a parameter that defines the star formation efficiency. In the models presented here each burst starts with an initial star formation efficiency  $\epsilon$  and with successive bursts having initial efficiencies reduced by a factor  $n$  (number of the burst). We call these: *attenuated burst models*. We have run models with three different initial star formation efficiencies,  $\epsilon$ : 0.64 (model M1),  $\epsilon = 0.33$  (M2) and  $\epsilon = 0.10$  (M3). The code calculates the chemical

abundances of 15 different elements as a function of time at different ages in steps of  $\Delta t = 0.5$  Myrs, from  $t = 0$ , to  $t = 13.2 Gyr$ s that would be the age of the assumed galaxy. Once the chemical evolution is calculated, the spectrophotometric properties corresponding to the whole stellar population are obtained, including the ionizing continuum of the stellar burst last formed. This continuum is introduced in the photo-ionization code together with its calculated abundances to calculate the properties of the ionized gas which is assumed to be at a distance  $R = 500$  pc and to be of constant density.

### 3 Results.

#### 3.1 Star formation rate (SFR).

The SFR is one of the main differences among models since it leads the behavior of all the other quantities. In Fig.1 we can see the SFH for our models. In all of them the first burst is intense, while the successive bursts are weaker because the amount of gas available for the next burst has decreased, in spite of the gas ejected by the evolving massive stars, and due to the attenuation of the efficiency included in the inputs. [3] have estimated the SFRs for a sample

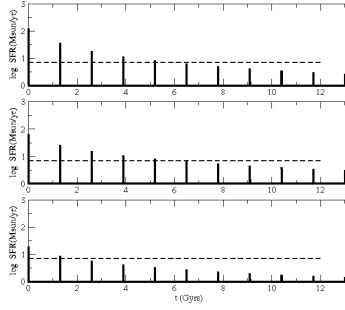


**Fig. 1.** Star formation rate of model M1 (upper panel), model M2 (middle one) and models M3 (bottom panel)

of 39 local HII galaxies of different morphologies from [13], being in the range from 0.5 to 7  $M_{\odot}/yr$ . Our models cover this range, whose upper bound is given by the broken line in the figure, during the five firsts bursts in M1 and M2 and after the second burst in M3.

#### 3.2 Evolution of the oxygen abundance.

The value of the oxygen abundance, which defines the metal content of stars and gas, increase with time due to the ejection of processed gas from massive stars. Observational data from [14] and [4] show that most HII galaxies have

gas oxygen abundances between  $7.5 < 12 + \log(O/H) < 8.5$ . We show these limits in Fig.2 as dashed lines. In this figure it can be seen that M1 reaches values over the upper limit of the observations right since the occurrence of the first burst. The efficiency of this first bursts is very high, forming a great number of stars, and then the metallicity grows rapidly. M2 and M3 show oxygen abundances in this range during the whole evolution due to the progressive attenuation of the bursts that makes the star formation smoother so that the oxygen abundance does not reach values as high as in M1.

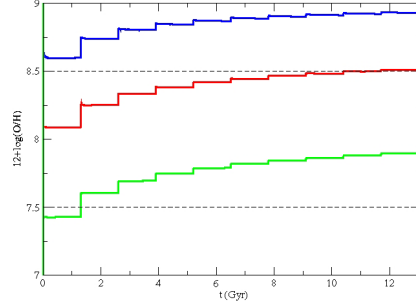


**Fig. 2.** Evolution of the oxygen abundance along 13.2 Gyrs M1(blue), M2(red), M3(green).

According to these results, the best models will be those with efficiencies in the range  $0.10 < \epsilon < 0.33$ . From now on we will analyze only these two types of models.

### 3.3 Emission lines: diagnostic diagrams

Once we have calculated the SED of the ionizing continuum, we have applied the photo-ionization code to obtain the emission lines intensities. Fig. 3 shows the  $[OIII]/H\beta$  vs the  $[OII]/H\beta$  relation. Our models seem to reproduce the tendency shown by data [4, 6], with M2 following the high excitation boundary of the data. However, the bulk of the data show values of the  $[OII]/H\beta$  ratio higher than computed. It should however be taken into account that all our models end up with the most recent burst. Therefore, from the point of view of gas ionization, the model regions are unevolved.

### 3.4 Equivalent width of $H\beta$

In Fig.4a) we have represented the equivalent width of  $H\beta$  vs the U-V color along the evolution of the galaxy for the successive star bursts of M2. When a burst occurs the  $EW(H\beta)$  is high and then decreases as the stellar population ages. We have over-plotted the results for SSPs from Starburst99 [8] with two

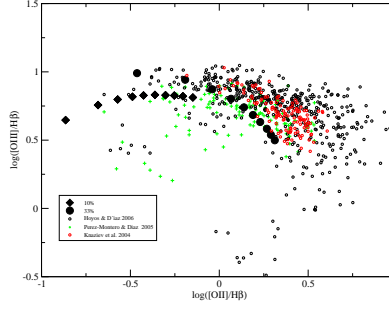


**Fig. 3.** Diagnostic diagrams comparing results from M2 and M3 with observational data from [4, 12, 6]

different metallicities (left panel). In order to compare our model results with observations, and since data on  $EW(H\beta)$  vs U-V color are scarce, we have used those from [4], based in a pseudo-color computed from the intensities of the adjacent continuum to the  $[OII]\lambda 3727$  and  $[OIII]\lambda 5007$  lines, producing a similar graph (right panel). The trend of data is reproduced by our models, while this is not the case for the SSP's. The black line in the left panel, that represents a low metallicity SSP, does not reach the red U-V colors shown by data nor the low values of  $EW(H\beta)$  observed for some HII galaxies. In order to decrease  $EW(H\beta)$  and to obtain bluer colors, a more metal-rich SSP might be selected (red line at the left panel), but such high abundance is inconsistent with observations, as we have already shown in Fig.2. Therefore, the observed trend cannot be explained as either an age effect (low metallicity SSPs do not reach  $EW(H\beta)$  values lower than  $100\text{\AA}$  and do not reproduce the colors), or a metallicity effect (high metallicity SSPs are not observed in HII galaxies). It is necessary to include both effects simultaneously, as we have done, to see how the effect of an underlying population, that contributes to the color of the continuum making it redder than expected, arises.

## 4 Conclusions

We have constructed models combining chemical evolution, evolutionary synthesis and photoionization, in a self-consistent way, to reproduce observational data of HII galaxies from different works. Galaxies with 1 Kpc size, total mass of  $10^8 M_\odot$  and a bursting star formation with different efficiencies are modeled. Models with efficiencies higher than  $\epsilon=0.33$  and lower than  $\epsilon=0.10$  are not consistent with observed oxygen abundances and SFHs. The models reproduce the tendency of the observations in the  $[OIII]/H\beta$  vs  $[OII]/H\beta$  diagram following the high excitation boundary shown by data. The equivalent width of  $H\beta$  line vs U-V color shows that is necessary to include underlying populations in order to reproduce the tendency of the observations, shifted to red

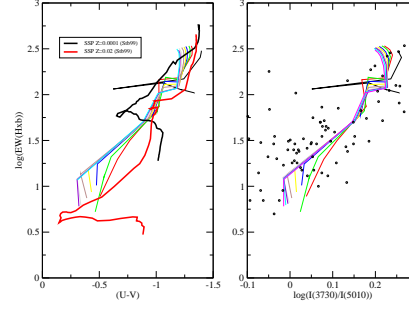


**Fig. 4.** *Left:* M2 equivalent width of the H $\beta$  line versus (U-V) color, compared with SSPs from [8]. *Right:* Same, but comparing with compare with observational data from [14]

colors, not only due to a metallicity increase, but also to the contribution from the previous bursts continuum. Future work will include a complete grid of models with different attenuations and intermediate efficiencies to reproduce the whole set of HII galaxies data, and the application of these models to other kinds of galaxies, like luminous compact blue galaxies, which might be reproduced by the most efficient star formation models.

## References

1. Cair6s, L. M., Garc6a-Lorenzo, B., Caon, N., V6lchez, J. M., Papaderos, P. & Noeske, K. , Ap&SS, 284(2003)
2. Ferrini, F., Matteucci, F., Pardi, C. & Penco, U., ApJ, 387 (1992)
3. Hoyos, C., Guzm6n, R., Bershad, M., Koo, D. & D6az, A. I., AJ, 128(2004)
4. Hoyos, C. & D6az, A. I., MNRAS, 365 (2006)
5. Garcia-Vargas, M. L., Bressan, A. & D6az, A. I., A&ASS, 112 (1995)
6. Kniazev, A., Pustilnik, S., Grebel, E., Lee, H. and Pramskij, A., ApJs, 153(2004)
7. Legrand, F., A&A, 354 (2000).
8. Leitherer, C. , Schaerer, D., Goldader, J., Delgado, R. M. G., Robert, C. , Kune, D. F., de Mello, D. F., Devost, D. & Heckman, T. M., ApJs , 123(1999)
9. Moll6, M., Ferrini, F. & D6az, A. I., ApJ, 466 (1996)
10. Moll6, M., Hardy, E. & Beauchamp, D., ApJ, 513 (1999)
11. Moll6, M., Ferrini, F. & Gozzi, G., MNRAS, 316(2000)
12. Perez-Montero, E. & D6az, A. I., VizieR Online Data Catalog, 736 (2005)
13. Telles, E., Melnick, J. & Terlevich, R., MNRAS, 288 (1997)
14. Terlevich, R., Melnick, J., Masegosa, J., Moles, M. & Copetti, M. V., A&ASS, 91 (1991)
15. Thuan, T. X., Izotov, Y. I. & Lipovetsky, V. A, ApJ, 445 (1995)
16. Thuan, T. X. & Izotov, Y. I., ApJ, 627 (2005)
17. Tolstoy, E., Ap&SS, 284 (2003)